# Computation of resonant frequency of annular microstrip antenna loaded with multiple shorting posts

M. Mahajan, S.K. Khah, T. Chakarvarty and A. De

**Abstract:** Shorting post loaded annular microstrip antenna is of considerable interest. Recent works have presented formulations for annular microstrip patch with a shorting post located at the centre of a circular disc, thereby converting the structure to an annular ring with a centre shot. A theoretical formulation for multiple post loading (up to ten posts) of an annular patch is presented. The posts are located away from the centre of the patch and are thin in diameter with respect to the diameter of the ring. The formulation accurately predicts resonant frequency. For an accurate formulation, the shorting posts have been considered as inductive impedances at the frequency of interest. It is shown that for a short loaded ring, $TM_{01}$ is the dominant mode. The simple tool presented can be suitably modified to incorporate switching diodes or varactor diodes.

## 1 Introduction

Shorting posts in microstrip antennas have recently come into use in order to take advantage of then different properties such as dual frequency, tunability and compactness [1–3]. Different geometries are being studied for different applications [4–6] of shorted antennas. Triangular and square patch microstrip antennas with shorting posts were studied for dual frequency operation and to enhance the bandwidth [7–9]. Miniaturised shorting-post microstrip antennas were presented in [10], where eigen frequencies and eigen modes were calculated for shorted circular patch. A circular microstrip antenna loaded with a single or concentrically located multiple shorting posts was studied in [11, 12]. Different methods were utilised to short the antenna surface with the ground planes, by using a hybrid active circulator [13] or via-holes [14–15]. A circular disc antenna with off-centred shorting posts was first proposed by De [16]. In this, a treatment is developed for single or multiple posts when the posts are symmetrically located, that is, equi-spaced along the circumference of the circle, concentric with the patch radiator. For a single post, symmetry is maintained when $\phi = 0°/180°$ that is, the post is located in the same line as that connecting the feed point and the centre of the patch. It was shown that the resonant frequency for each mode depends on $t = r_2/r_1$, where $r_2$ is the radial distance of the posts from the centre of the patch and $r_1$ the radius of the patch. The resonance also depends on the ratio $t_2 = r_1/\Delta$, where $\Delta$ is the post radius. As the posts move towards the edge of the patch, the resonance frequency of $TM_{11}$

mode first increases and then drops. This effect is more pronounced when the number of posts $P$ is large. The lowest resonance for post-loaded patch was shown to be of (0,1) mode. The higher order modes like (0,2) and (1,2) show interesting results. For both these modes, there exists a critical value of $t$ where the resonance frequency is the same as that of the unperturbed patch. On both sides of this radial distance, the resonance frequency increases.

In recent times, two major works have been reported for shorted ring antenna. In [17], an approximate analysis of a short-circuited ring-patch antenna at $TM_{01}$ mode is presented based on the cavity model. Analytical expressions for resonance frequency, fields, radiation pattern and input impedance based on this model have been developed. In [18], short-circuited ring-patch antennas working at $TM_{01}$ mode based on neural networks are studied. The dependence between the fundamental antenna parameters, such as internal radius ($r$), the external radius ($R$) and permittivity of the substrate ($\varepsilon$), has been studied.

In light of the above discussions, it is seen that significant amount of work needs to be done for shorting-post loaded annular microstrip antenna. An accurate model of such an antenna is necessary to predict the various performances of the antenna. Theoretical modelling for an annular ring loaded with multiple posts is not reported in the literature and is therefore attempted in the present work. This analysis may lead to a practical design where the shorting posts are replaced by switching diodes positioned symmetrically about the feed. A pair of switching diodes can be electronically switched on or off based on the operating frequency desired. In the following analysis a theoretical basis for the loading effect of multiple posts at the same radial distance from the centre of the annular patch is formulated. In previous articles, shorted-post loaded circular patch antennas had been analysed. In this article, the same method is extended to obtain resonance frequencies for an annular ring when multiple posts are loading the ring at a certain radial location. Theoretical results are compared with simulated results (IE3D) as well as with measured results.

## 2 Theoretical analysis

The analysis is based on the cavity model in which it is assumed that the substrate is electrically thin ($h \ll 0$). The electric field within the substrate has only $z$-components and is non-variant in the $z$-direction. The magnetic field has essentially $x$ and $y$ components. The basic ring geometry with shorting posts is shown in Fig. 1. The annular ring of inner radius '$a$' and outer radius '$b$' is loaded with '$P$' number of passive conducting posts of radius $\Delta$ at angular locations $\phi_i$ ($i = 1, 2, \ldots, P$) on the circumference of a concentric circle of radius '$c$' where $a < c < b$. The given annular ring in the presence of the source can be considered as consist of two half discs where the line of axis is through the feed point and the centre of the patch.

For region I ($a < r < c$), the expressions for the electric and magnetic fields are obtained as

$$E_z^{(1)} = -j\omega_{np}\mu\{C_1 J_n(k_{np}r) + C_2 N_n(k_{np}r)\}\cos n\phi \quad (1)$$

$$H_r^{(1)} = -\left(\frac{n}{r}\right)\{C_1 J_n(k_{np}r) + C_2 N_n(k_{np}r))\}\sin n\phi \quad (2)$$

and

$$H_\phi^{(1)} = -k_{np}\{C_1 J_n'(k_{np}r) + C_2 N'(k_{np}r)\}\cos n\phi \quad (3)$$

where $J_n(k_{np}r)$ is the Bessel function of the first kind of order $n$, $\omega_{np}$ and $k_{np}$ are the angular frequency and propagation constant, respectively, for the $TM_{np}$ mode, and $C_1$ and $C_2$ are constants. Prime denotes a derivative with respect to its argument. The integer '$n$' corresponds to the order of the Bessel function and '$p$' denotes the $p$th zero of $Jn'(k_{np}r)$. The subscript '$z$' is ignored for a particular mode identification as the electric field is non-variant along the $z$-direction.

Similarly for region II ($c < r < b$), the expressions for electric and magnetic fields are obtained as

$$E_r^{(2)} = -j\omega_{np}\mu\{C_3 J_n(k_{np}r) + C_4 N_n(k_{np}r)\}\cos n\phi \quad (4)$$

$$H_r^{(2)} = -\left(\frac{n}{r}\right)\{C_3 J_n(k_{np}r) + C_4 N_n(k_{np}r)\}\sin n\phi \quad (5)$$
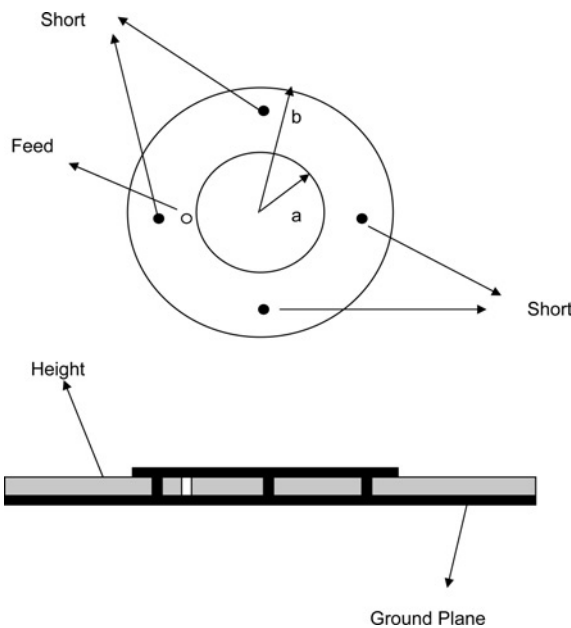


**Fig. 1** *Geometry of annular Microstrip patch antenna loaded with shorting post*

and

$$H_\phi^{(2)} = -k_{np}\{C_3 J_n'(k_{np}r) + C_4 N_n'(k_{np}r)\}\cos n\phi \quad (6)$$

where $C_3$ and $C_4$ are constants and $N_n(k_{np}r)$ is the Bessel function of the second kind.

Applying the vanishing tangential component of the magnetic field in the two regions at the boundary edges leads to the modification of field expressions as follows

$$E_z^{(1)} = -j\omega_{np}\mu C_n^{(1)} F_n^{(1)}(k_{np}r)\cos n\phi \quad (7)$$

$$H_\phi^{(1)} = -k_{np} C_n^{(1)} F_n'^{(1)}(k_{np}r)\cos n\phi \quad (8)$$

and

$$E_z^{(2)} = -j\omega_{np}\mu C_n^{(2)} F_n^{(2)}(k_{np}r)\cos n\phi \quad (9)$$

$$H_\phi^{(2)} = -k_{np} C_n^{(2)} F_n'^{(2)}(k_{np}r)\cos n\phi \quad (10)$$

where

$$F_n^{(1)}(kr) = J_n(k_{np}r)N_n'(k_{np}a) - J_n'(k_{np}a)N_n(k_{np}r)$$

$$F_n^{(2)}(k_{np}r) = J_n(k_{np}r)N_n'(k_{np}b) - J_n'(k_{np}b)N_n(k_{np}r)$$

and

$$F_n'^{(1)}(k_{np}r) = J_n'(k_{np}r)N_n'(k_{np}a) - J_n'(k_{np}a)N_n'(k_{np}r)$$

$$F_n'^{(2)}(k_{np}r) = J_n'(k_{np}r)N_n'(k_{np}b) - J_n'(k_{np}b)N_n'(k_{np}r)$$

It is assumed that the diameter of the circular post is small. Such a thin post can be assumed to be replaced by a conductor in the form of a circular arc strip having arc length equal to the diameter of the post $2\Delta$ coincident with a circle of radius $c$. For an arc strip of small arc length, the axial current may be assumed to be uniform along its width. This current per unit width is given as $E_z/Z_0$ where $Z_0$ is the impedance per unit length of the post. The impedance per unit length of such a post, carrying uniform current and connected between two conducting discs, is given as [19]

$$Z_0 = \frac{\eta k}{4}\left[1 - J_0^2(kc) + j\left\{\frac{2}{\pi}\ln\left(\frac{2}{\gamma k\Delta}\right) + J_0(kc)N_0(kc)\right\}\right] \quad (11)$$

where $c$ is the radial distance of the post from the centre of the patch.

The expression derived by Sengupta [19] assumes an axially oriented metallic post in an infinite radial waveguide ($\rho = \infty$), which sustains only $E$-type radial modes. Use of this expression in conjunction with the theory developed in [12] reveals that this particular model is accurate for all modes of loaded ring resonator when the post is not very close to the edge of the patch. Deviations are observed when the posts are moved to the edge. A possible solution to this is suggested in [20]. In this, the shunt posts are characterised using the planar waveguide model in which sidewalls are replaced with a fictitious 'perfect magnetic conductor'. The presence of the magnetic walls makes it necessary to consider the reflected field components, which are generated by the infinite array of imaged multipoles located at the points.

In the proposed model of the loaded annular ring, the impedance expression derived in [19] has been utilised. However, to compensate for the edge effects, an empirically generated correction factor is also incorporated. It has been shown in a previous publication that such a combination

2

*IET Microw. Antennas Propag., Vol. 2, No. 1, February 2008*

leads to a very accurate model of the post-loaded circular patch [21]. The correction factor is given as

$$\text{CF} = \frac{\sin\left(\pi/2\varepsilon_n\right)\left\{\left|J_0(P/4V)\right|\right\}^{2P}}{J_0(\alpha t_d)^{(D/2)-0.7}J_0(t_d)^2 J_0\left((c - a_e/a_e)\right)^2} \quad (12)$$

where $t_d = (c - b_e)/b_e$, where $b_e$ is the effective radius of the ring due to fringing fields.

$$D = 4 \text{ for } P \leq 4.$$
$$\text{Else}$$
$$D = p$$

$$V = \left(\frac{R_P}{Q_P}\beta_n + \alpha_n R_P\right)$$

where

$$\alpha_n = 0 \quad \text{for } n = 0 \text{ else } 1;$$
$$\beta_n = 1 \quad \text{for } n = 0 \text{ else } 0;$$

$Q_i$ and $R_i$ values are obtained from Table 1.

$$\varepsilon_n = 1 \quad \text{for } n = 0 \text{ and } \varepsilon_n = 2 \text{ for } n \neq 0$$

To compute the resonance frequency, the impedance expression used is therefore

$$Z_0 = \frac{j\omega\mu}{2\pi}\left\{\ln\left(\frac{2}{\gamma k\Delta}\right) + \frac{\pi}{2}J_0(kc)N_0(kc)\right\}CF = X_T \quad (13)$$

The empirical correction factor correctly predicts the effect of multiple posts on the fringe of annular ring for up to ten posts.

The electric and magnetic fields given by (7)–(10) satisfy the following boundary conditions.

$$E_z^{(2)} = E_z^{(1)} \quad \text{at } r = c \quad (14)$$

$$H_\phi^{(2)} - H_\phi^{(1)} = \frac{\sum_{i=1}^{P} E_z^{(2)}}{(Z_0 \cdot 2\Delta)} \quad \text{at } r = c \quad \text{for } \phi_i - \frac{\alpha}{2} < \phi < \phi_i + \frac{\alpha}{2} \quad (15)$$

where $\alpha$ is the angle subtended by the shorted post at the centre of the ring cavity. The summation over index '$i$' indicates that the boundary condition is applicable for all shorting posts.

From (14) and (15), it is found that

$$\frac{C_n^{(2)}}{C_n^{(1)}} = \frac{F_n^{(1)}(k_{np}c)}{F_n^{(2)}(k_{np}c)} \quad (16)$$

## Table 1: Correction factor values

| No. of posts | $Q_i$ | $R_i$ |
|---|---|---|
| 1 | 0.3 | $0.12\,\varepsilon_n$ |
| 2 | 0.55 | $0.35\,\varepsilon_n$ |
| 3 | 0.6 | $0.6\,\varepsilon_n$ |
| 4 | 0.6 | $0.9\,\varepsilon_n$ |
| 5 | 1.0 | 2.0 |
| 6 | 1.05 | 2.5 |
| 7 | 1.0 | 3.0 |
| 8 | 0.95 | 3.5 |
| 9 | 0.9 | 4.5 |
| 10 | 0.85 | 5.0 |

and

$$\frac{C_n^{(2)}}{C_n^{(1)}} = \frac{F_n'^{(1)}(k_{np}c)}{F_n'^{(2)}(k_{np}c) - F_n^{(2)}(k_{np}c)} \quad (17)$$
$$\sum_{i=1}^{P}(j\omega\mu/2X_i k_{np}c\varepsilon_n\pi)[1 + \cos(2n\phi_0)]$$

Now using (16) and (17)

$$\frac{F_n'^{(2)}(k_{np}c)}{F_n^{(2)}(k_{np}c)} - \frac{F_n'^{(1)}(k_{np}c)}{F_n^{(1)}(k_{np}c)} - \sum_{i=1}^{P}\frac{\varepsilon_n(1 + \cos(2n\phi))}{2\,k_{np}cX_T} = 0$$

$$(18)$$

The resonance frequency for a given mode '$np$' is obtained by solving (18), where integer '$n$' denotes the order of Bessel's function and '$p$' corresponds to the $p$th zero of (18).

## 3 Numerical results

In this article, a theoretical model is developed made to analyse the annular ring resonator with multiple shorting pins (posts). The structure is loaded with multiple shorting posts that are distributed uniformly. The results of the annular ring with varying number of posts are compared with simulated results obtained from MoM-based commercial solver IE3D. For the analysis of the resonator, the dimensions chosen are $a = 30$ mm, $b = 60$ mm, $c = 50$ mm, $h = 1.59$ mm and $\varepsilon_r = 2.2$. For analysis, the number of posts is varied from 1 to 10. For every case, the angular distance of the posts on the ring is constant (e.g. for $P = 9$, the angular separation among the shorts on ring is $2\pi/9$). The variation in resonance frequency with the radial location of the short is also calculated for different modes ($n = 0, 1, 2$) and for $P = 1$, as shown in Fig. 2. For comparison, the same results are plotted with simulated data. The simulated and numerical values are in very good agreement. In the dominant mode ($n = 0$), the maximum predicted error is less than 1%, and in higher order modes ($n = 1, 2$) the maximum predicted error is 2–3%. The resonance frequency changes with the number of posts. The variation in resonance frequency is also computed for dominant and higher-order modes ($n = 0$,
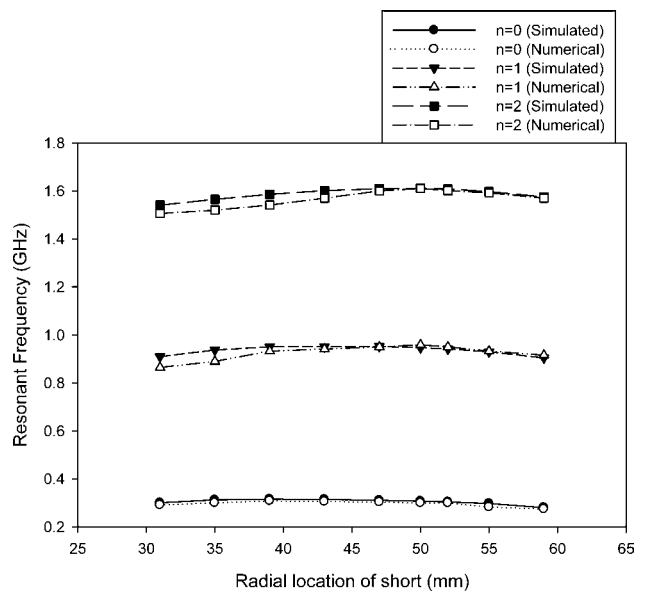


**Fig. 2** *Comparison of present theory with simulated data: resonant frequency with radial location of short (a = 30 mm, b = 60 mm, h = 0.159 mm, $\varepsilon_r$ = 2.2, P = 1)*
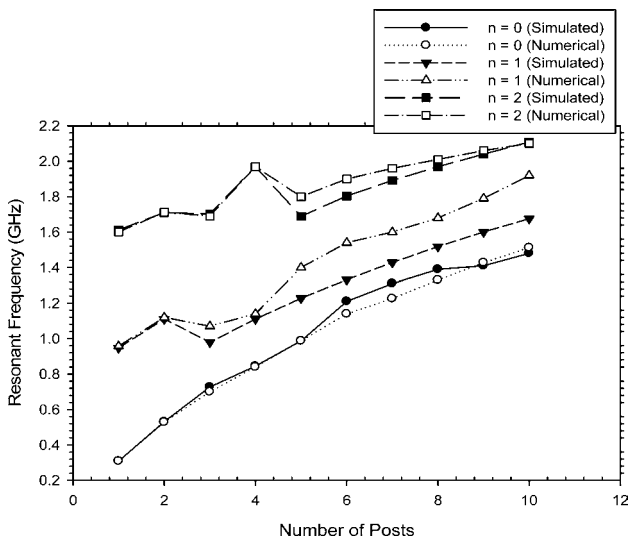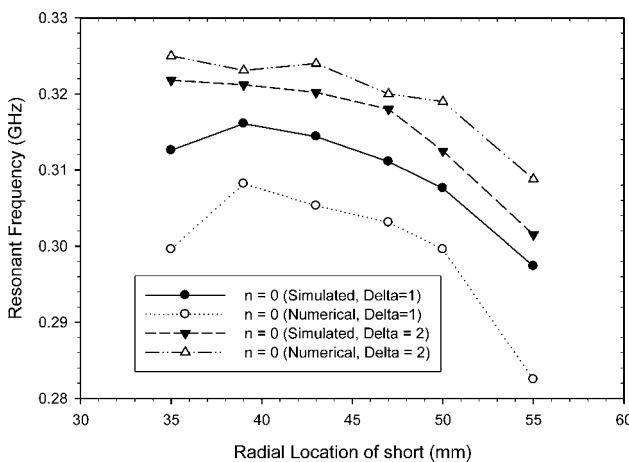
**Fig. 3** *Comparison of present theory with simulated data: resonant frequency with number of posts (a = 30 mm, b = 60 mm, c = 50 mm, h = 0.159 mm, $\varepsilon_r$ = 2.2)*

1, 2) with a number of posts. Fig. 3 shows that the simulated and numerical values are in very good agreement. The maximum error in prediction is 2–3%. The resonance frequency is also varied with the radial location of the short by changing the radius of the pin ($\Delta$ = 1, 2 mm). The variation of resonance frequency with radial location for different $\Delta$ in dominant mode (for n = 0) is shown in Fig. 4. The numerical results show a good agreement with the simulated results. The error for $\Delta$ = 1 mm is 2%, whereas the error for $\Delta$ = 2 mm is 3–4%. A similar variation is also calculated for a higher mode, shown in Fig. 5, (for n = 1). The numerical and simulated results are in complete agreement. The maximum error when $\Delta$ = 1 and 2 mm is 2–3%.

## 4 Measured results

The results numerically calculated by the present model are used for the practical design of the ring resonator and a comparison is being done between the measured and numerical results. The design parameters of the antenna are chosen as a = 30 mm, b = 60 mm, c = 50 mm, h = 1.59 mm, $\varepsilon_r$ = 2.2 and $r_0$ = 35 mm, where $r_0$ represents the location of the feed point. The numbers of posts for the measured



**Fig. 4** *Comparison of present theory with simulated data: resonant frequency with radial location of short for dominant mode (n = 0) for different $\Delta$ = 1 mm, $\Delta$ = 2 mm. (a = 30 mm, b = 60 mm, h = 0.159 mm, $\varepsilon_r$ = 2.2, P = 1)*
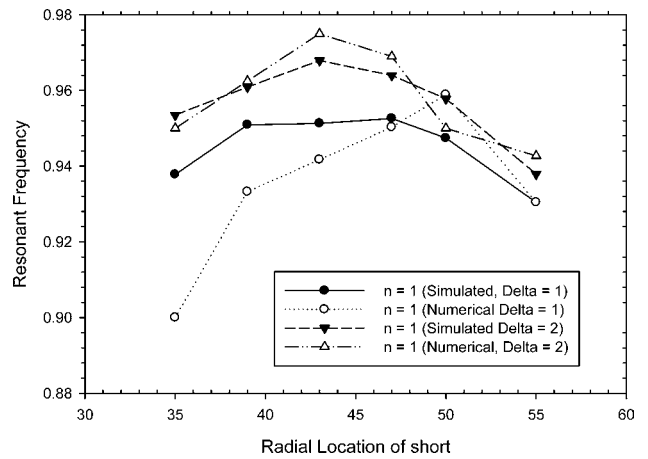


**Fig. 5** *Comparison of present theory with simulated data: resonant frequency with radial location of short for higher order mode (n = 1) for different $\Delta$ = 1 mm, $\Delta$ = 2 mm. (a = 30 mm, b = 60 mm, h = 0.159 mm, $\varepsilon_r$ = 2.2, P = 1)*
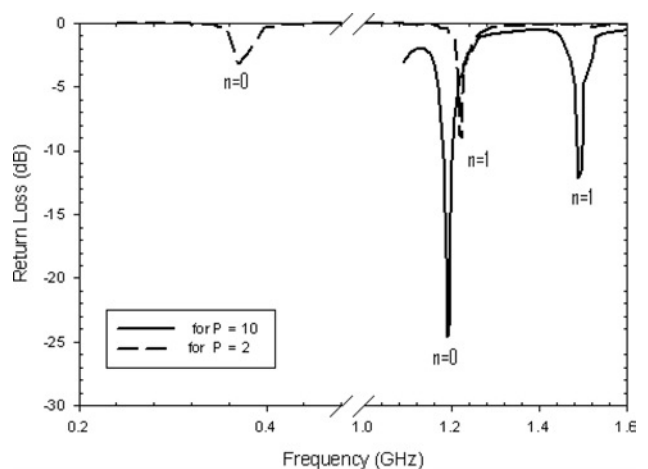
**Table 2:** **Measured values of return loss of antenna at different modes with different posts**

| No. of posts | Measured return loss, dB | | |
| --- | --- | --- | --- |
| | n = 0 | n = 1 | n = 2 |
| 1 | −2.103 | −3.762 | −6.53 |
| 2 | −3.07 | −5.0 | −8.7 |
| 4 | −15.8 | −5.9 | −10.3 |
| 10 | −3.58 | −23.7 | −13.27 |

results are 1, 2, 4 and 10. The measured results of return loss are given in Table 2. For two and ten posts, the plot of measured values of return loss is also shown in Fig. 6. The comparison between measured and numerically calculated values of resonant frequencies for first three modes (n = 0, 1 and 2) is shown in Table 3. Both numerical and measured results are in good agreement. The error percentage is less than 3%.

## 5 Discussion

The model developed and presented in this article gives a reasonably accurate prediction of resonance frequencies



**Fig. 6** *Variation of return loss with frequency for different no. of posts (a = 30 mm, b = 60 mm, c = 50 mm, h = 0.159 mm, $\varepsilon_r$ = 2.2)*

4

*IET Microw. Antennas Propag., Vol. 2, No. 1, February 2008*

**Table 3: Comparison of measured and computed values of resonant frequency of shorted ring resonator**

| No. of posts | Resonant frequency, GHz | | | | | |
| --- | --- | --- | --- | --- | --- | --- |
| | $n = 0$ | | $n = 1$ | | $n = 2$ | |
| | Computed | Measured | Computed | Measured | Computed | Measured |
| 1 | 0.214 | 0.2198 | 0.6678 | 0.6706 | 1.113 | 1.133 |
| 2 | 0.376 | 0.37 | 0.787 | 0.79 | 1.19 | 1.22 |
| 4 | 0.60 | 0.6127 | 0.79 | 0.7884 | 1.36 | 1.388 |
| 10 | 1.036 | 1.072 | 1.44 | 1.4 | 1.738 | 1.74 |

for a shorted patch annular ring antenna. As highlighted before, a circular patch with a centre shot can also be considered an annular ring with a shorted inner wall. However, in our model the inner wall is not shorted and thin shorting pins are located within the ring to perturb the field patterns of the given excited mode. The analysis tool considers a probe-free region where natural resonances are obtained for the given structure. The probe location affects the input impedance seen by the coaxial probe for a given mode. In [22], such impedance had been calculated for different probe locations for a circular patch. The same method can be extended to obtain the input impedance for a shorted annular ring. Similar is the case of radiation pattern. In this case, the pins are symmetrically located. So, intuitively, it can be suggested that cross-polarisation is not degraded by the loading of pins. However, a metallic pin incurs a small amount of power loss. Therefore gain of the antennas will be reduced.

## 6 Conclusion

In this article, a method to compute the resonance frequency of an annular microstrip antenna loaded with multiple shorting posts is presented. The resonance frequency for the dominant mode and other higher-order modes is predicted with accuracy. Numerical and simulated results show a very good agreement. $TM_{01}$ is the dominant mode for a short-loaded ring antenna. This analysis can be further extended to incorporate switching diodes or varactor diodes.

## 7 References

1 Waterhouse, R.B.: 'Small microstrip patch antennas', *Electron. Lett.*, 1995, **31**, pp. 604–605
2 Waterhouse, R.B., Targonski, S.D., and Kokotoff, D.M.: 'Improving the mechanical tolerances and radiation performance of shorted patches', Proc. IEEE Antennas Propagation Society Int. Symp., 1997, **3**, pp. 1852–1855
3 Sanad, M.: 'Effect of the shorting posts on short circuit microstrip antennas', Proc. IEEE Antennas and Propagation Society Int. Symp., 1994, **2**, pp. 794–797
4 Chakravarty, T., and Sanyal, S.K.: 'A novel microcontroller-programmable circular microstrip antenna', *Microw. Opt. Technol. Lett.*, 2000, **25**, (6), pp. 383–387
5 Payne, A.N.: 'Improved bandwidth and efficiency of short antennas by the use of radials'. Proc. Ninth Int. Conf. on HF Radio Systems and Techniques, (Conf. Publ. No. 493), 2003, pp. 210–215
6 Wang, Y.J., and Lee, C.K.: 'Compact and broadband microstrip patch antenna for the 3G IMT-2000 handsets applying Styrofoam and shorting posts', *Prog. Electromag. Res.*, 2004, **47**, pp. 75–85
7 Chow, Y.D.S., Tuan-Yung, H., and Row, J.S.: 'Dual-frequency shorted triangular patch antenna'. Proc. Asia-Pacific Conference APMC-2005, 2005, vol. 4, pp. 4–7
8 Lu, J.H., Tang, C.L., and Wong, K.L.: 'Novel Dual frequency and broad band designs of slot loaded equilateral triangle microstrip antennas', *IEEE Trans. Antenna Propag.*, 2000, **48**, pp. 1048–1054
9 Deshmukh, A.A., and Kumar, G.: 'Compact broadband gap-coupled shorted square microstrip antennas', *Microw. Opt. Technol. Lett.*, 2006, **48**, pp. 1261–1265
10 Porath, R.: 'Theory of miniaturized shorting–post microstrip antennas', *IEEE Trans. Antenna Propag.*, 2000, **48**, (1), pp. 41–47
11 Lin, Y., and Shafai, L.: 'Characteristics of concentrically shorted circular patch microstrip antennas', *IEE Proc., Microw. Antennas Propag.*, 1990, **137**, pp. 18–24
12 Chakravarty, T., and De, A.: 'Design of tunable modes and dual-band circular patch antenna using shorting posts', *IEE Proc., Microw. Antennas Propag.*, 1999, **146**, (3), pp. 224–228
13 Gupta, S., Nath, P.K., and Sarkar, B.K.: 'Integrated microstrip shorted antenna using hybrid active circulator'. Proc. Asia-Pacific Conf. APMC-2000, 2000, pp. 719–722
14 Kouzaev, G.A., Deen, M.J., Nikolova, N.K., and Rahal, A.H.: 'Cavity models of planar components grounded by via-holes and their experimental verification', *IEEE Trans. Microw. Theory Tech.*, 2006, **54**, pp. 1033–1042
15 Yan, Z.: 'A microstrip patch resonator with a via connecting ground plane', *Microw. Opt. Technol. Lett.*, 2000, **32**, pp. 9–11
16 De, A.: 'Studies on rectangular and circular patch radiators', PhD thesis, Indian Institute of Technology, Kharagpur, 1985
17 Posadas, V., Vargas, D., Iglesias, E., Roy, J., and Pascual, M.: 'Approximate analysis of short circuited ring patch antenna working at $TM_{01}$ mode', *IEEE Trans. Antennas Propag.*, 2006, **54**, (6), pp. 1875–1879
18 Teruel, O., and Iglesias, E.: 'Design of short circuited ring patch antennas working at $TM_{01}$ mode based on neural networks', *IEEE Antennas Wirel. Propag. Lett.*, 2006, **5**, pp. 349–352
19 Sengupta, D.L., and Martins-Camelo, L.F.: 'Theory of dielectric-filled edge-slot antennas', *IEEE Trans. Antennas Propag.*, 1980, **28**, (4), pp. 481–490
20 Finch, K.L., and Alexopoulas, N.G.: 'Shunt posts in microstrip transmission lines', *IEEE Trans. Microw. Theory Tech.*, 1990, **38**, (11), pp. 1585–1594
21 Chakravarty, T., and De, A.: 'Resonant frequency of a shorted circular patch with the use of a modified impedance expression for a metallic Post', *Microw. Opt. Technol. Lett.*, 2002, **33**, (4), pp. 252–256
22 Chakravarty, T., and De, A.: 'Using cavity model analysis for design of dual-band dual-slant-polarized microstrip antenna', *Microw. Opt. Technol. Lett.*, 2003, **37**, (5), pp. 331–337

*IET Microw. Antennas Propag., Vol. 2, No. 1, February 2008*

5